

**CHAMBERED NAUTILUS SHELL
STRESS ACCOMMODATION
MECHANISMS**

Peter Drlik
Bob McReynolds
Dr. Albert Your

10 December, 2002

Submitted in partial fulfillment of course requirements
for MatE 210, Experimental Methods in Materials Engineering
Fall 2002

Professor Guna Selvaduray

CHAMBERED NAUTILUS SHELL
STRESS ACCOMMODATION
MECHANISMS

Peter Drlik
Bob McReynolds
Dr. Albert Your

10 December, 2002

ABSTRACT: The macroscopic architecture of the mollusk *Nautilus Pompilius* is analyzed with finite element analysis and the microstructure is evaluated with scanning electron microscopy to understand the stress accommodation mechanisms that allow the thin lightweight shell to withstand daily pressure migrations of over fifty atmospheres.

The finite element analysis of a simplified geometry of the shell graphically represents how hydrostatic pressure applied externally to the shell is translated into stress and deformation throughout the structure. The curved internal septa of the shell are demonstrated to provide elastic flexibility to the structure by bending to accommodate the external compressive environment. It is predicted that this bending could ultimately result in fracture at the septum to wall joint as a result of hydrostatic pressure of deep seawater depending on orientation of the lamellae of the nacreous structure in this region.

Scanning electron microscope images show orientation of the platelets on the septum, but poor sample preparation precludes any conclusions about platelet design at the critical stress area of the septum to wall joint.

TABLE OF CONTENTS

Abstract	ii
Table of Contents	iii
List of Figures	iv
I. INTRODUCTION	1
II. FINITE ELEMENT ANALYSIS	
A. EXPERIMENTAL METHODS	3
FEA Software	3
The Model	3
The Simplified Model	4
The Environment	7
B. RESULTS	8
III. SCANNING ELECTRON MICROSCOPY	
A. EXPERIMENTAL METHODS	10
B. RESULTS	11
IV. DISCUSSION	17
V. CONCLUSION	21
VI. ACKNOWLEDGEMENTS	22
REFERENCES	22

LIST OF FIGURES

FIGURE 1	Cross section of chambered nautilus shell	p. 4
FIGURE 2	Symmetries of nautilus shell	p. 5
FIGURE 3	Internal horseshoe shape of nautilus shell	p. 6
FIGURE 4	Simplified ProE model of nautilus shell	p. 6
FIGURE 5	The living nautilus	p. 7
FIGURE 6	Von Mises stress in the shell model at 1000 psi	p. 8
FIGURE 7	Convergence of FEA model	p. 9
FIGURE 8	Location of cross section for SEM pictures	p. 10
FIGURE 9	Gold Coated SEM sample surface	p. 10
FIGURE 10	Shell growth overlap boundary	p. 12
FIGURE 11	Overlap boundary at 2222 X Magnification	p. 12
FIGURE 12	Fractured septum at 33 X Magnification	p. 13
FIGURE 13	Fractured septum at 119 X Magnification	p. 14
FIGURE 14	Superficial striations and underlying platelet formation	p. 15
FIGURE 15	Platelet formation at 3948 X Magnification	p. 15
FIGURE 16	Septum to shell joint at 3733 X Magnification	p. 16
FIGURE 17	Principle stresses in nautilus shell at 2200 fsw	p. 18
FIGURE 18	Comparison of Von Mises diagrams exposing versus protecting outer septum to 1000 psi	p. 19

I. INTRODUCTION

The micro-structural and compositional similarities between mammalian bone and a material called nacre, which is commonly found in mollusk shells have spawned several arms of research into various aspects of nacre over the last decade. Micro-structural architectures of both mammalian bone tissue and nacre consist of brittle inorganic microstructures embedded in a tougher, but softer organic matrix. One field of research that has emerged from observation of the nacreous structure is the bio-chemical construction of dissimilar material matrices. Bio-chemical processes that mollusks use to construct nacre are being mimicked in development of self-assembling semiconductor devices⁽¹⁾, but may also be of benefit to advance structural materials development. Other researchers have focused on the implications of this architecture on mechanical properties of the material, and more specifically on fracture toughness mechanisms on the micro-structural scale^(2,3). From this perspective, nacre is attractive because the materials work-of-fracture is nearly three orders of magnitude greater than that of monolithic ceramics, while the organic matrix consists of only 5% of the material by volume⁽⁴⁾. The other 95% is inorganic calcium-carbonate (CaCO_3) platelets approximately five nanometers wide and $\frac{1}{2}$ of a nanometer thick arranged in either a columnar or sheet ordered pattern depending on the specific mollusk. Similar micro-structural architectures are being replicated with metallic materials for structural applications⁽⁵⁾.

The shell of the mollusk *nautilus pompilius*, which is commonly referred to as the chambered nautilus because of its unique and elegant architecture, is composed of nacre. The platelet matrix structure of nacre makes it an inherently non-isotropic

material, which is a factor that must be considered when attempting to replicate the microstructure in advanced composites design. Traditional bulk material machining methods are not adequate for creating complex shapes in non-isotropic materials. The objective of this study is to correlate the macro-structural architecture of the chambered nautilus mollusk with the micro-structural nacreous platelet arrangements in the context of the living organism's natural environmental demands. An understanding of the how the material is micro-structurally arranged can lead to an understanding of how the material is constructed. A simplified Finite Element Analysis is proposed to determine the stress states and elastic deformations that occur in the nautilus shell during its daily migrations of up to 2000 feet⁽ⁱ⁾ of seawater which correlates to over 50 atmospheres of hydrostatic pressure. Calcium Carbonate platelet orientation within the nacre of the shell is then observed using scanning electron microscopy and correlated to the stress states in the geometry.

A non-fresh Nautilus Pompilius shell approximately eight inches in diameter, purchased from **Capitola Seashells** in Capitola, California served as the geometrical model for the Finite Element Analysis. The same shell was sectioned for the scanning electron microscopy pictures. A non-fresh specimen was sufficient for this study because the specimen was used only for the purposes of geometrical modeling and for imaging of microstructures. This study did not include any mechanical testing methods that would have required fresh specimens due to the impact of water content as in previous research⁽⁵⁾.

ⁱ 2000 feet of seawater is the depth suggested by the Monterey Bay Aquarium on their website.

II. FINITE ELEMENT ANALYSIS (FEA)

A. EXPERIMENTAL METHODS

Pro/Mechanica Software Program

There are many software tools available for performing Finite Element Analysis of structures. For this study, the student version of the Pro/Engineering (ProE) 3-D Modeling with Pro/Mechanica FEA software package by PTC was selected for its flexibility and availability. The ProE package was at the time of this study limited to performing only linear elastic analysis so yield strengths and plastic deformations could not be accounted for. This was not a hindrance since the objective of the study was to model the elastic behavior of the material during daily migrations of 2000 feet of seawater. Nonetheless, this limitation must be considered in observation of the data.

The Model

The chambered nautilus architecture was determined by Raup in 1967 to be described by fundamentally three dimensions named Whorl Expansion Rate, Degree of Overlap and Shape. Saunders and Shapiro elaborated on this description in their evaluation of shape on hydrostatics in 1986 ⁽⁶⁾. These concepts were used as a foundation for the geometrical model of this study. A complete shell model would be created by sweeping an elliptical shell cross-section through a logarithmic spiral. The radial dimensions of the ellipse are increased as the ellipse is swept outward from the center of the spiral to accommodate the organism as it grows. As the living nautilus organism grows it extends its external elliptical shell along the spiral path

and leaves semi-parabolic internal septa behind it at a rate of approximately one per month as shown in a photograph of the shell cross section in Figure 1. The fact that both the external walls and the internal septa are secreted by the organism simultaneously as it grows suggests that the orientation of the planes of calcium carbonate platelets in the nacre would be parallel to the internal surfaces of each structure.



**FIGURE 1: Cross Section of the Chambered Nautilus
(Picture from website of www.sciencemall-usa.com)**

The Simplified Model

The geometrical model used for the study simplifies the complete shell structure by taking advantage of symmetries and approximate symmetries to establish constraints and reduce computer resource requirements. There is an obvious mid-plane symmetry through the shell that defines the cross section pictured

in Figure 2. This defines one surface that can be sectioned and restrained from moving in the direction perpendicular to the photo, hence called direction z .

The cross section in Figure 2 can then be divided into approximate quarterly symmetries, defining two more planes that can be sectioned and restrained from moving in the x and y directions respectively as well as the z direction for both planes. Finally, symmetry along the radial direction can also be approximated from the larger outer chambers to the smaller inner chambers to cut out the internal chamber section and constrain the internal surface of the model in the x , y , and z directions.

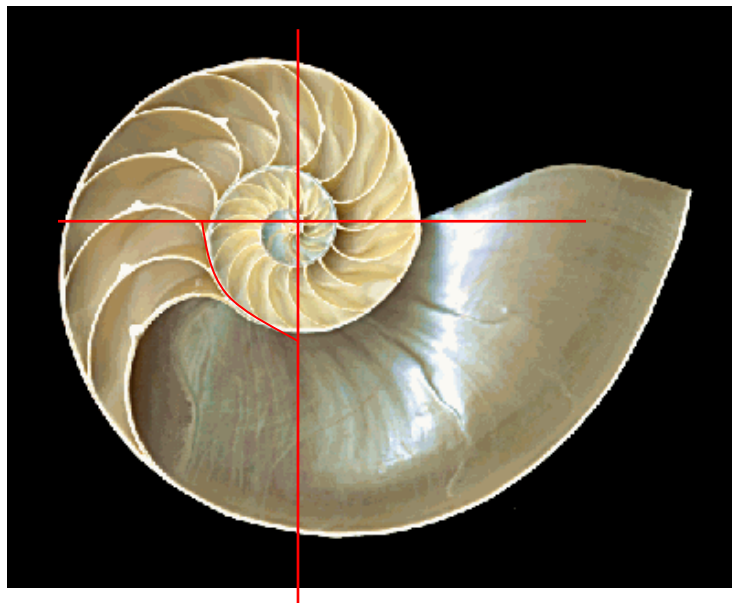


FIGURE 2: Approximate symmetries of the Chambered Nautilus
(Picture from website of www.sciencemall-usa.com)

The final simplification that is made is that the internal surface of the shell section is flat in the model rather than horseshoe shaped as shown in Figure 3. This is done simply to minimize computer resource requirements and is estimated to not

detrimentally skew results. The resulting ProE model with constraint directions is shown in Figure 4.



Figure 3: Top view of the horseshoe shape of the internal chambers of the nautilus

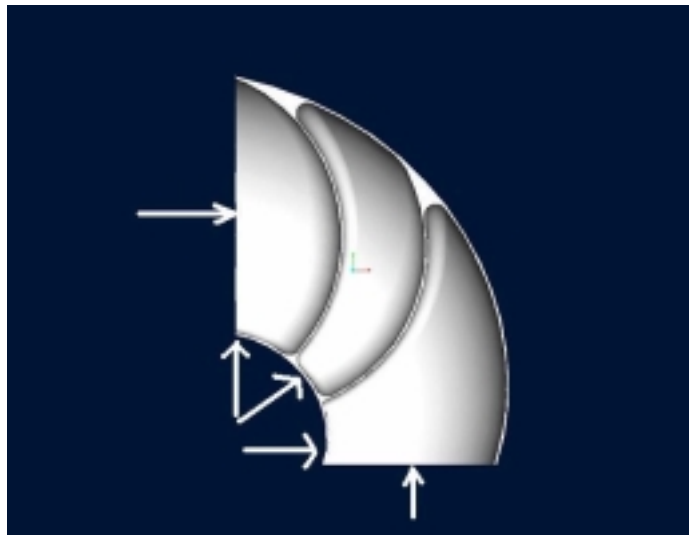


Figure 4: Side view of the simplified nautilus shell ProE Model with FEA Constraint Directions.

The Environment

The living mass of the nautilus resides within the largest chamber at the outside of the spiral as shown in Figure 5. The nautilus is capable of filling the rest of the chambers with either seawater or gas through osmosis to control its buoyancy and migrate vertically through depth of seawater. During the daytime, the temperature sensitive nautilus migrates to the ocean floor to escape the increased temperatures that result from the sun heating the water closer to the surface. At night, the nautilus rises to within 200 feet of seawater (fsw) from the cooler ocean surface to feed on plankton. The osmosis mechanism is only functional up to a depth of approximately 700 fsw. The nautilus utilizes another propulsion mechanism to migrate deeper than 700 fsw and can, in some situations, get as deep as 2000 fsw. This implies that below 700 fsw, the structure of the shell must support the pressure difference between the inside of the shell and the external hydrostatic pressure.



Figure 5: The living nautilus (Picture from the website of the Environmental Science and Geography Department at William Paterson University, Wayne, New Jersey)

B. RESULTS

The Analysis

A pressure of 1000 psi simulating 2200 fsw (1000 psi X 33 fsw / 14.7 psi) was applied to the external surface of the shell in the first model. The value of Young's Modulus used for nacre in the model was 70 GPa, as stated by Wang et al ⁽⁶⁾. Though the 70 GPa value was stated for fresh abalone and pearl oyster nacre, the structures are similar enough to justify the use of this value. Figure 6 shows that the maximum Von Mises stress that occurs in the material is approximately 35,000 psi (~240 MPa)ⁱⁱ along the edges where the septum joins the external wall.

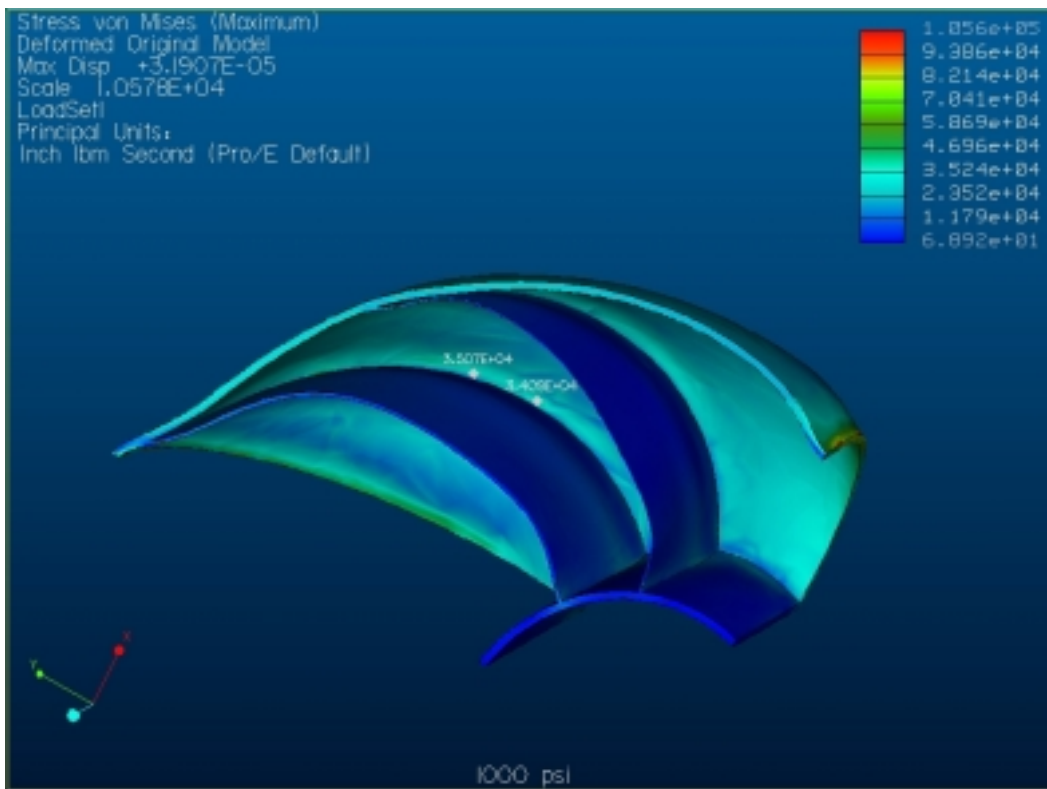


Figure 6: Von Mises Stress in the Model at 1000 psi (2200 fsw)

ⁱⁱ Note that the high Von Mises stresses that appear on the upper right edge of the model can be ignored as this edge would normally be supported by another rib.

The ProE/ ProMechanica student software package provides an animation of the deformation under load so that proper constraints can be verified by witnessing the movements of the edges of the model. Unfortunately, the student version of the software automatically generates the element mesh and does not provide access to the model meshing application so it is not possible to see or modify the mesh. Nonetheless, rather than regenerating finer meshes in iterations until convergence of results is attained as is done in some FEA applications, ProMechanica instead uses the same element mesh through iterations, but it increases the order of polynomial on each successive iteration until the specified convergence is attained. Thus, a convergence chart such as Figure 7 can be used to verify adequate iterations have been performed.

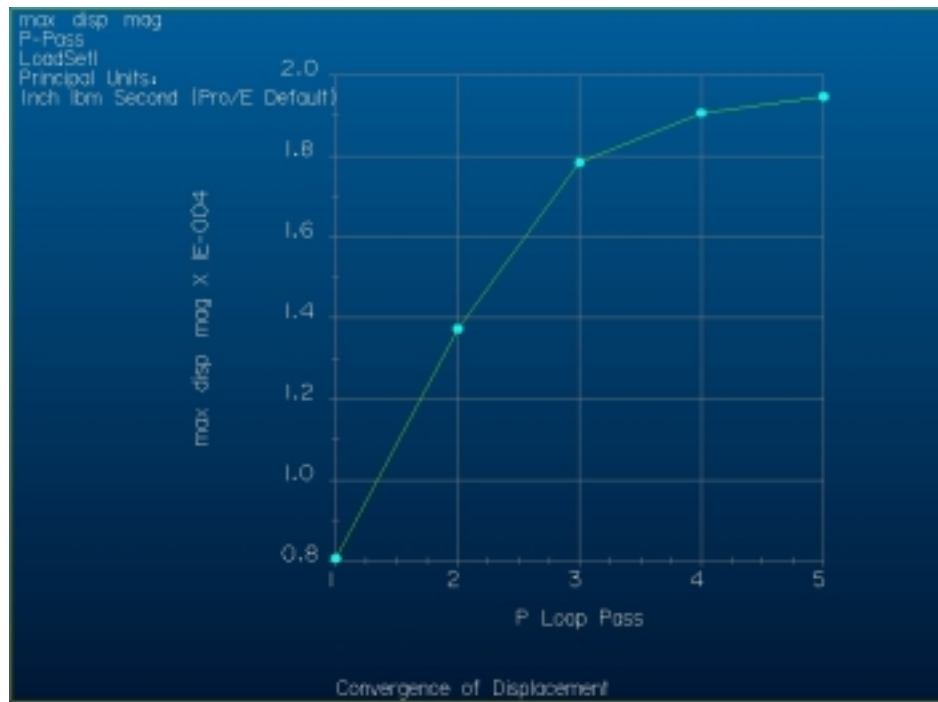


Figure 7: Convergence of Displacement meeting the 10% specified convergence after 5 passes.

III. SCANNING ELECTRON MICROSCOPY

A. EXPERIMENTAL METHODS

Specimen Preparation

The nautilus shell specimen was sectioned through plane AA with a saw. The resulting section plane surface of the smaller section was polished down to 1 micron with alumina paste and sputtered with a 30 nm layer of gold using a Pelco SC-7 Auto Sputter Coater. The resulting specimen, shown in Figure 8, was then taped to the SEM stage with Carbon tape.

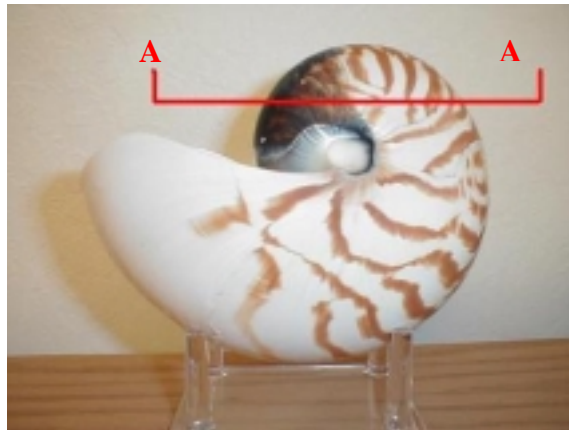


Figure 8: Nautilus shell specimen and cross section for SEM pictures.



Figure 9: Gold coated inspection surface.

Images of the gold coated surface were taken with a Philips XL40 scanning electron microscope at the Microscope and Graphics Imaging Center at California State University in Hayward, California at various magnifications to evaluate platelet orientation with respect to the stress states predicted in the FEA model. This SEM has a resolution of approximately 2 nm.

B. RESULTS

Most of the polished and coated surface appeared featureless in the SEM at even the highest magnifications. However, regions where the shell was irregularly fractured during the sectioning process clearly revealed the platelet structure.

One interesting feature apparent in both the SEM and the optical microscope is the boundary line that delineates where this particular nautilus shell grows around itself in its spiral growth pattern. The location of this feature is identified at a lower magnification in Figure 10 and magnified in Figure 11. The specific features of this apparently fused boundary could not be detailed with this SEM. Further analysis with an Environmental SEM which does not require sputter coating or a higher resolution TEM would be required for a more detailed description of the micro-structure of this feature. Fine micro-cracks apparent in Figure 9 appeared parallel to most of this boundary region as well, but it is not clear whether these were the result of the sectioning process or if they were naturally occurring.

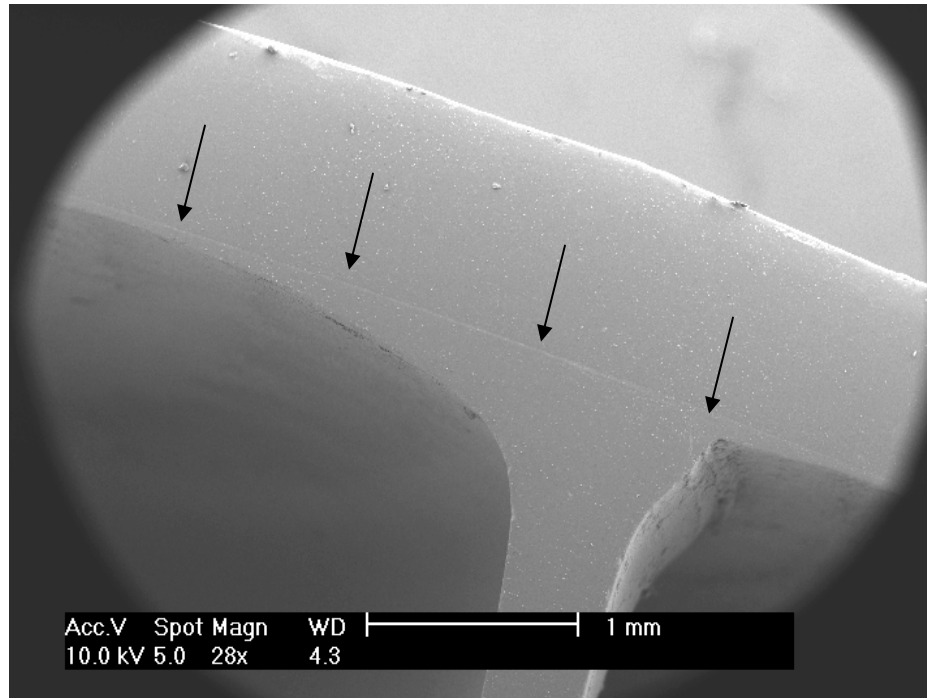


Figure 10: Boundary line of interior shell to exterior shell

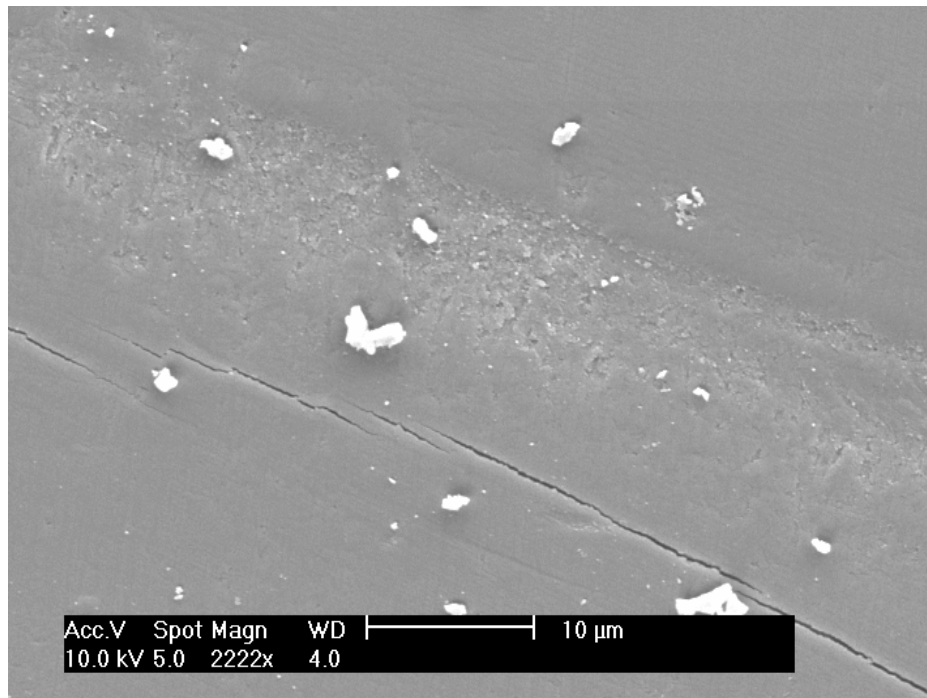


Figure 11: Boundary (pock mark area) at higher magnification showing microcracks that appear parallel to most of the boundary line.

Figure 12 shows a fractured septum that was not polished because it is recessed from the polished surface. The detail box, with a field of view of 6 microns, shows that the platelet structure is parallel to the septum surface.

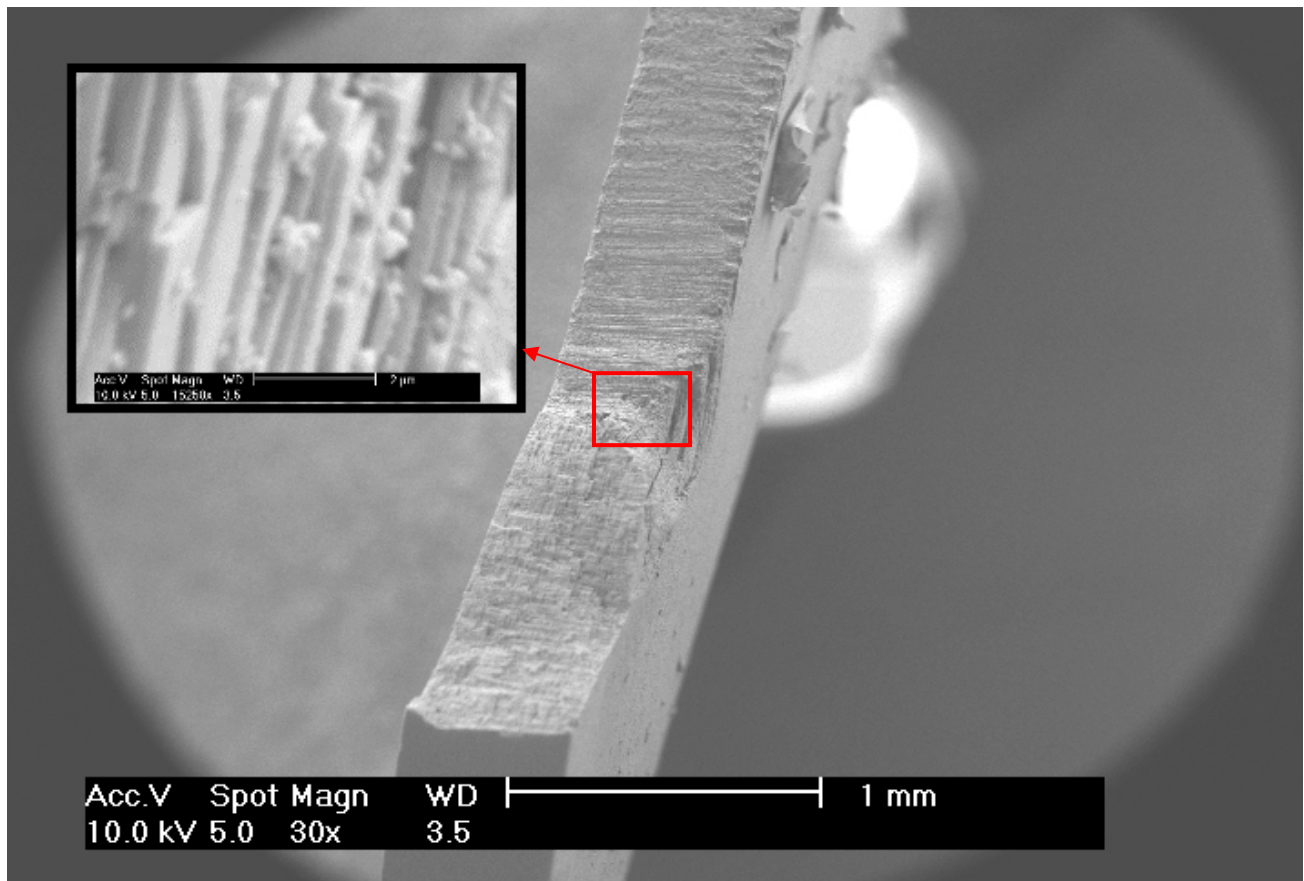


Figure 12: Fractured septum showing orientation of platelets. Inner box is 6 micron field of view.

Figure 13 is a higher magnification picture of the same septum section from Figure 12. It provides a clearer picture of the fracture surface. The horizontal striations on the septum toward the top of Figure 13 appear to be superficially induced by sample preparation methods. Similar superficial striations can be seen in Figure 14 as pointed

out by the arrows in the figure, though the underlying platelet orientation is much clearer at the magnifications of figures 14 and 15.

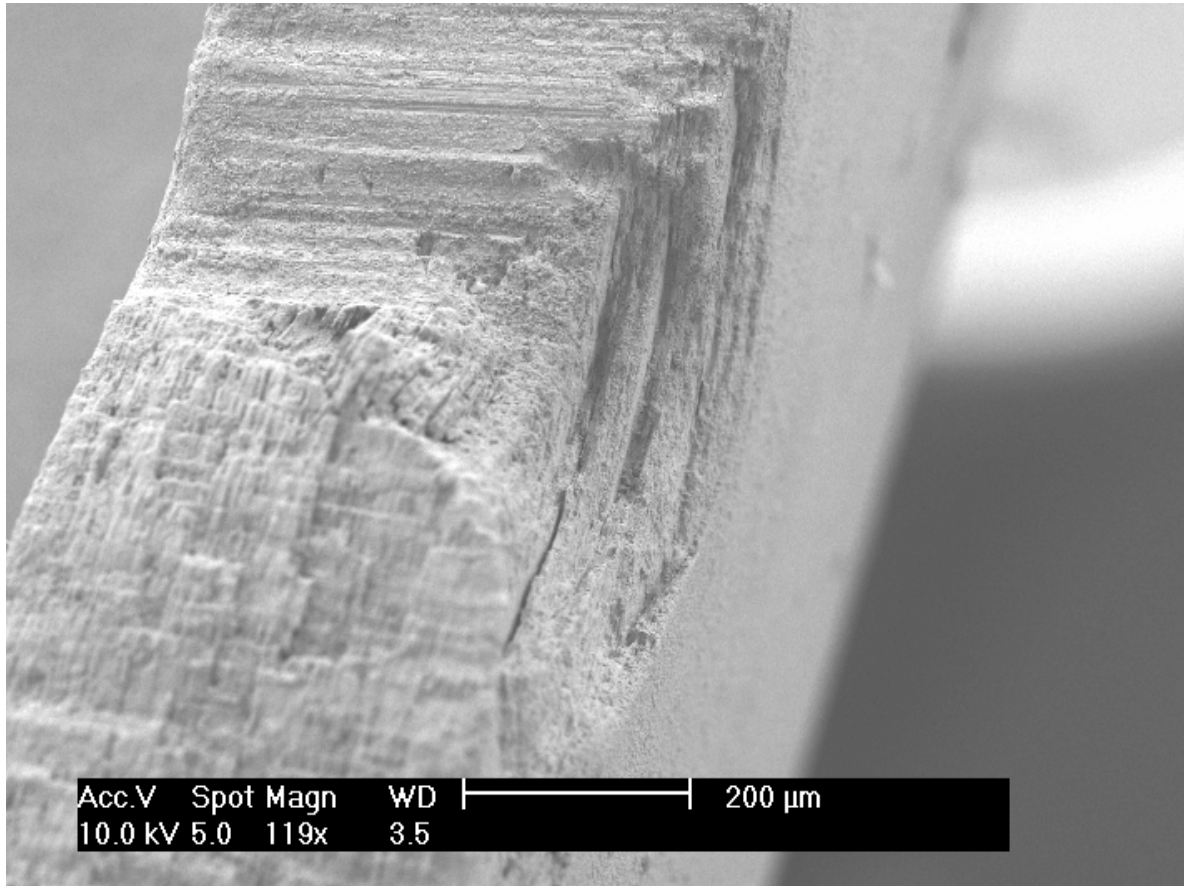


Figure 13: Fracture surface of septum showing bulk platelet orientation.

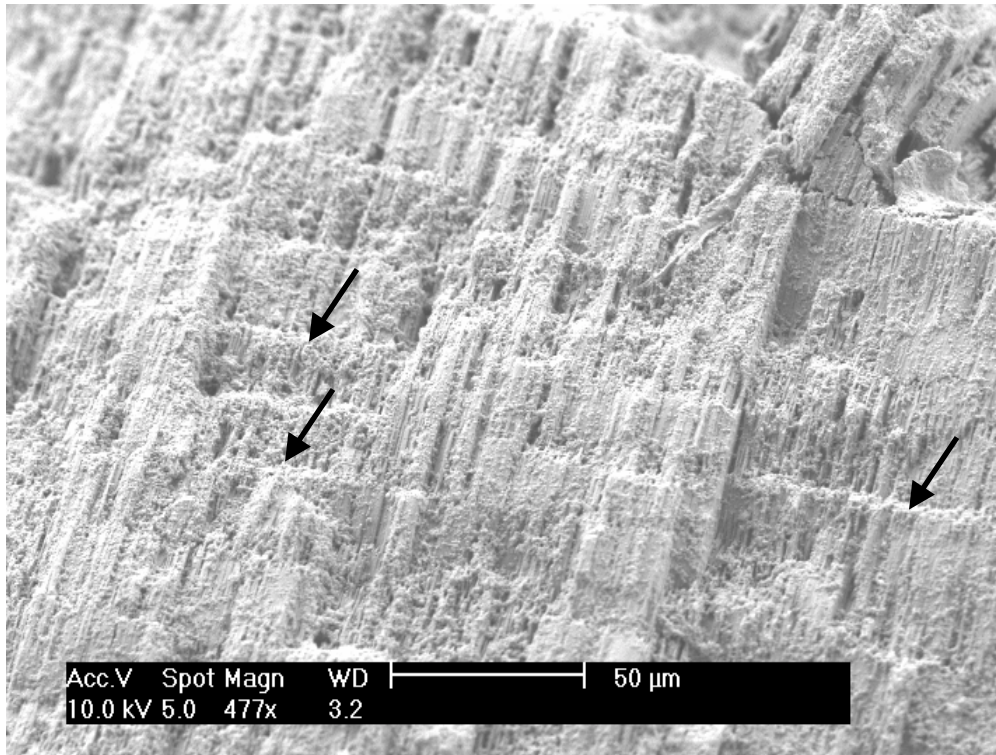


Figure 14: Superficial striations and underlying platelet orientation.

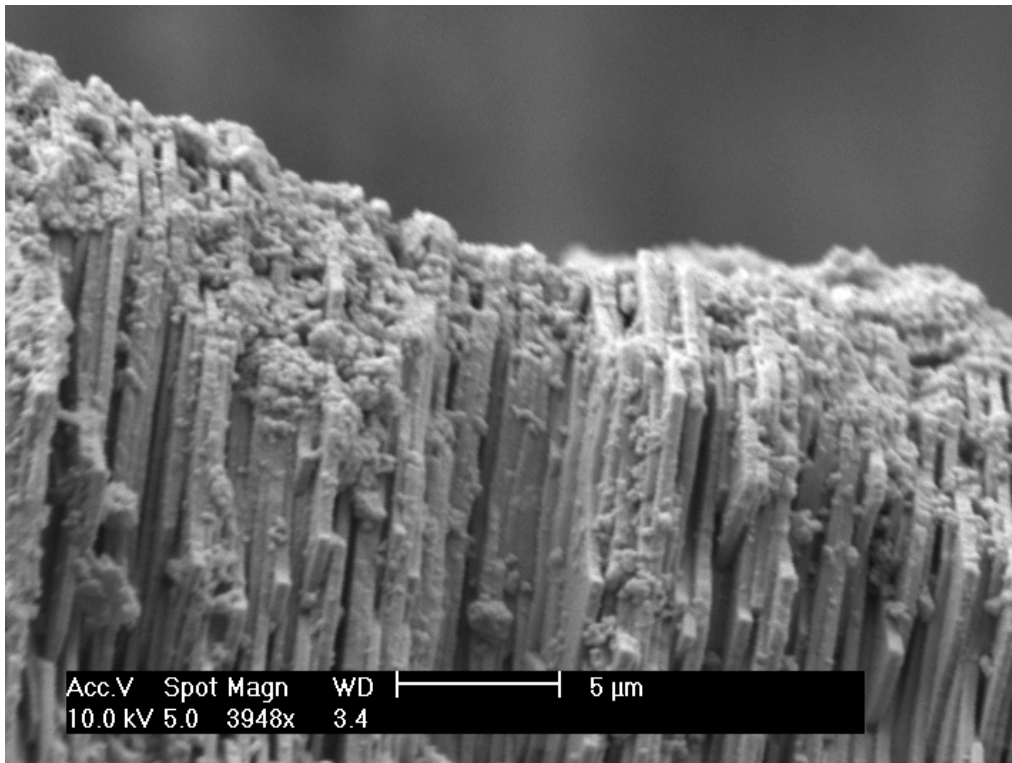


Figure 15: Higher magnification showing platelets (covered with residue)

One of the primary objectives of this study was to determine the platelet orientation in correlation to the stress states naturally encountered. The FEA showed that the stress states were highest at the location where the septum joins the external shell, so a high magnification picture was taken at a fractured surface where the septum joins the wall. This is shown in Figure 14. Though the platelet structure is clearly evident at this location, the extent of damage in the area precludes any conclusions about orientation of the structures.

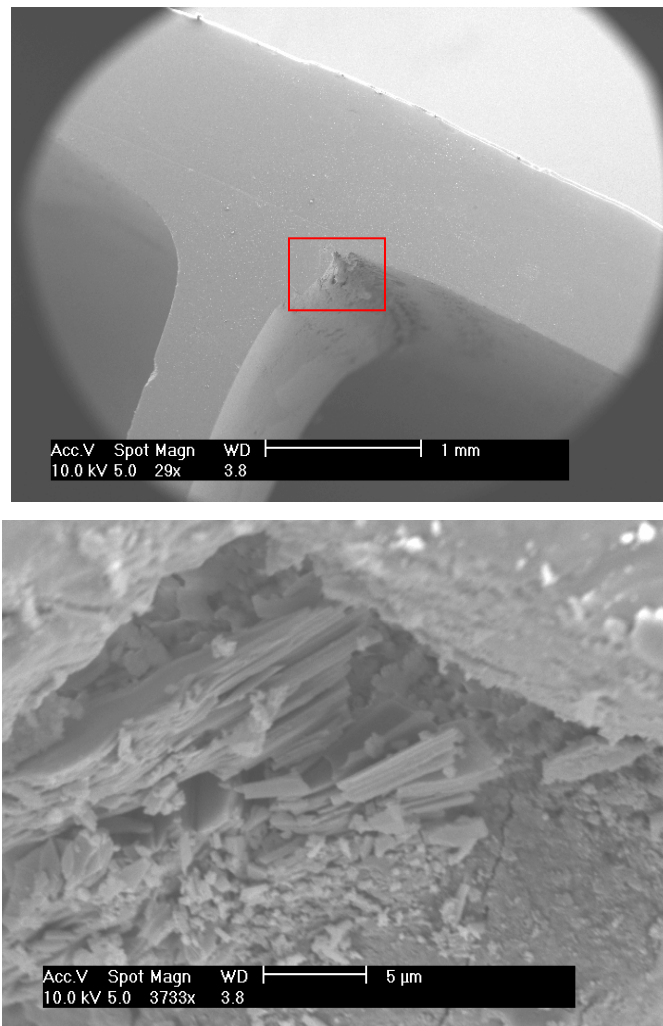


Figure 16: Damaged septum joint. Above; location. Bottom; high magnification.

IV. DISCUSSION

Wang et al ⁽⁶⁾ showed that the compressive strength of nacre, when the load is applied parallel to the lamellae was greater than 370 MPa, but only 160 MPa when the load is applied at a 45° angle to the lamellae. In tensile testing, the same study showed that inelastic deformation began between 105 MPa to 140 MPa depending on the type of nacre. The model in this study predicted a Von Mises stress of 240 MPa along the septum to shell joint at a depth of 2200 fsw which would exceed the limits of tensile elastic deformation for the material. The Von Mises stress provides an empirical relationship between the three principle stresses of a multi-axial stress environment in a coordinate system and the uni-axial yield strength of a material to determine if the material will inelastically deform in a multi-axial stress environment. The Von Mises stress is given by Equation 1 and when it exceeds the yield strength of the material, the material is predicted to fail ⁽⁷⁾.

$$\text{EQUATION 1: } \sigma_{\text{VM}} = \frac{1}{\sqrt{2}} \left[(\sigma_1 - \sigma_2)^2 + (\sigma_2 - \sigma_3)^2 + (\sigma_3 - \sigma_1)^2 \right]^{1/2}$$

From Equation 1, it is clear that the Von Mises stress is always a positive value and that it does not tell anything about whether principle stresses are tensile or compressive. Principle stress information can be determined by plotting the three separate principle stresses in ProMechanica as shown in Figure 17. The principle stresses at the septum-wall joint location of interest are shown to be mostly compressive;

$$\sigma_1 = +20.7 \text{ MPa (+3000 psi in ProMechanica)}$$

$$\sigma_2 = -137.9 \text{ MPa (-20000 psi in ProMechanica)}$$

$\sigma_3 = -206.8 \text{ MPa}$ (-30000 psi in ProMechanica)

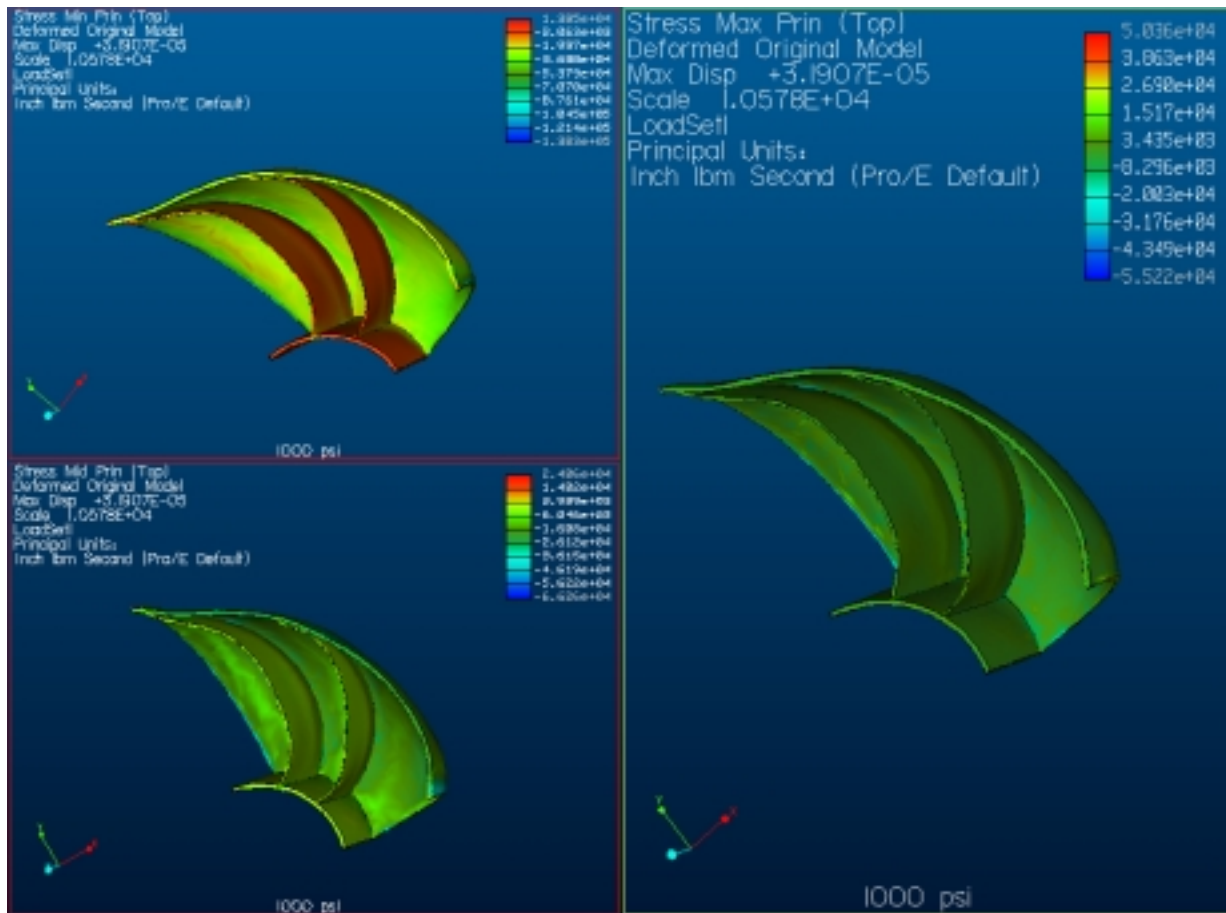


Figure 17: Principle Stresses in nautilus shell at 2200 fsw

The compressive yield strength of nacre was already stated to be between 160 MPa and greater than 370 MPa depending on orientation of the nacreous platelet structure. The principle stresses could potentially exceed this depending on platelet orientation at this location.

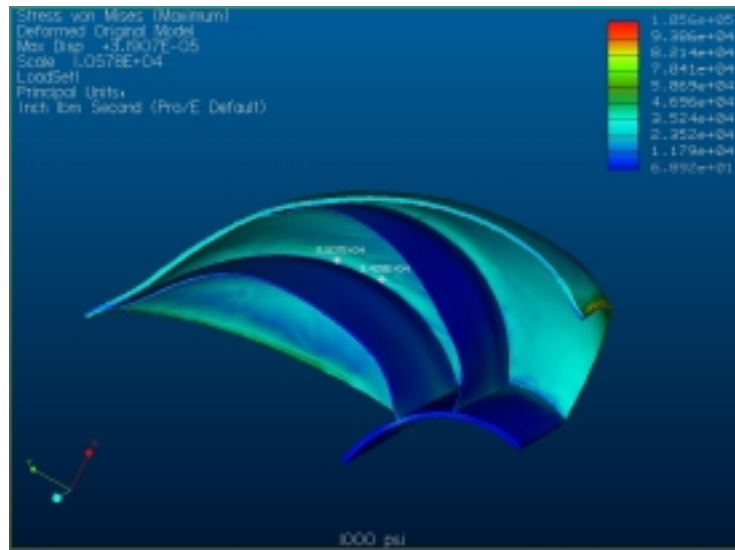
Scanning electron microscope pictures only revealed the orientation of the platelet structures near the midsection of the septum, which was already easily predicted by the nature of the septum construction. Improper sample preparation techniques precluded the observation of platelet orientation in the region of most interest, at the

high radius of curvature of the septum to wall joint. Additional investigation with a clean and fresh fracture surface in a high resolution SEM, Environmental SEM, or TEM at the septum to external shell joint would provide this information.

In 1977, Saunders and Wehman⁽⁸⁾ used resistance transducers to measure resistivity changes due to stress-strain states on the septum and the external shell of the nautilus while imploding the shell in a hyperbaric chamber. That study concluded that, at depth, the septum experiences a tensile stress state equal in magnitude to the compressive stress state of the external shell. This method exposed the outer septum of the shell to the hydrostatic pressure, though in a living nautilus, the outer septum is somewhat shielded from the pressure by the organism that resides in the outer chamber as shown in Figure 5. Exposing the outer septum to the hydrostatic pressure results in a very different stress state as realized by comparing the results previously shown of a protected septum in Figure 6 with the results of an exposed septum shown in Figure 17. The protected septum yields a maximum Von Mises stress of 230 MPa (35,000 psi) in the model, while the exposed septum yields a maximum Von Mises stress of 598 MPa (87,000 psi). This indicates that the exposed septum method in a hyperbaric chamber is not a realistic representation of real conditions and may underestimate the depth at which a shell would fail in nature.

Additionally, the strain gauge method used in that study appears to provide information about strain in only one direction at the location that each gauge is placed and the orientation of the strain gauge is not specified in the study. The stress-strain states in this model are more complex than can be determined with uniaxial strain gauges. For example, during a standard tensile test, tensile loads are applied in the

vertical direction of a specimen. If a strain gauge is attached in the proper vertical direction, then a corresponding positive strain is reported as the material is stretched along the vertical axis. However, if the strain gauge is attached to the specimen horizontally, a negative strain would be reported as the material contracts to conserve volume of the specimen. This negatively reported strain does not correspond to a compressive stress.



Results shown previously in Figure 6 for comparison to Fig. 17

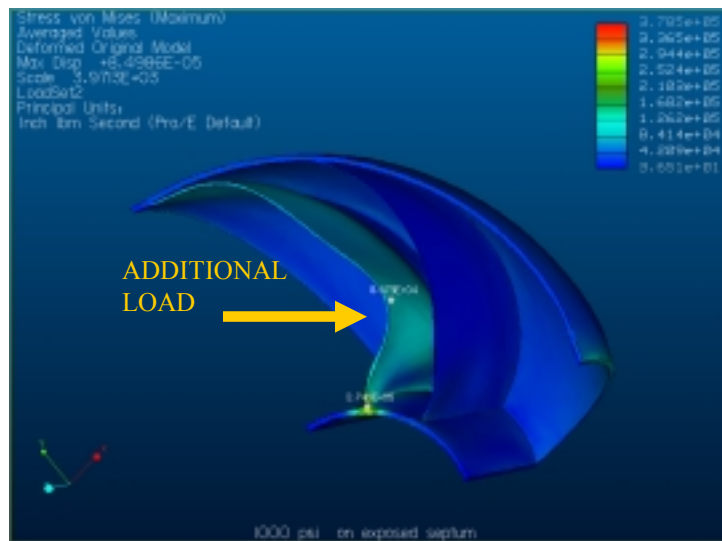


Figure 18: Effects of applying pressure to outer septum in addition to external shell.

V. CONCLUSION

The chambered nautilus uses a combination of macroscopic geometrical design features and microscopic material design to accommodate stresses encountered in its habitat. The macroscopic geometry of the shell of the chambered nautilus distributes hydrostatic pressure load effectively enough to allow the shelled creature to migrate over 2000 feet of seawater depth without inelastic deformation. The internal septa of the shell provide not only an effective buoyancy control mechanism as is commonly known, but they also provide flexible support to the structure during severe pressure migrations.

The orientation of the planes of the microscopic calcium carbonate platelets in the nacre material has been shown to be parallel to the internal surfaces of the septum, though the features of the platelet structure at the critical high angle septum-shell joint have not been detailed.

VI. ACKNOWLEDGEMENTS

The scanning electron microscope pictures in this report were taken on the Philips XL40 SEM at the Microscope and Graphics Imaging Center (MAGIC) at California State University in Hayward, California with the assistance of laboratory manager Melissa Carter and at IBM Research Center with the assistance of Walter Prater.

¹ Seung-Wuk Lee, Chuanbin Mao, Christine Flynn, Angela Belcher, *Ordering of Quantum Dots Using Genetically Engineered Viruses*, Science Magazine, May 3, 2002, p. 892-895

² J.D. Currey, P. Zioupos, P. Davies, *Mechanical Properties of Nacre and Highly Mineralized Bone*, Proceedings Royal Society of London – B, 268, pp. 107-111, 2001.

³ Song Fan, Bai Yilong, *Analysis of the Strengthening and Toughening of a Biomaterial Interface*, Science in China (Series A), Volume 44, #12, December 2001.

⁴ R.Z. Wang, Z. Suo, A.G. Evans, N. Yao, I.A. Aksay, *Deformation Mechanisms in Nacre*, Journal of Materials Research, Volume 16, #9, Sep 2001

⁵ C.H. Liu, Wen-Zhi Li, Heng-De Li, *TiC/ Metal Nacreous Structures and their Fracture Toughness Increase*, Journal of Materials Research, Volume 11, #9, p.2231, Sep 1996

⁶ W.B. Saunders, E.A. Shapiro, *Calculation and Simulation of Ammonoid Hydrostatics*, Paleobiology, Volume 12, Issue 1, pp. 64-79, Winter 1986

⁷ G.E. Dieter, *Mechanical Metallurgy*, 3rd edition, McGraw-Hill, 1986.

⁸ W.B. Saunders, D.A. Wehman, *Shell Strength of Nautilus as a Depth Limiting Factor*, Paleobiology, Volume 3, Issue 1, pp. 83-89, Winter 1977